ELSEVIER

Journal of Photochemistry and Photobiology A: Chemistry 146 (2002) 189–197

Journal of Photochemistry and Photobiology A:Chemistry

www.elsevier.com/locate/jphotochem

# Photocatalytic degradation of 4-nitrophenol in aqueous $TiO_2$ suspensions: Theoretical prediction of the intermediates

Nevim San, Arzu Hatipoğlu, Gülin Koçtürk, Zekiye Çınar*

*Department of Chemistry, Yıldız Technical University, 34210 Istanbul, Turkey*

Received 20 September 2001; accepted 25 October 2001

**Abstract**

The kinetics of the photocatalytic degradation of 4-nitrophenol (4-NP) in the presence of $TiO_2$ has been investigated experimentally and theoretically. The effects of the catalyst loading, the initial concentration of 4-NP, $H_2O_2$ and the added $Cu^{2+}$ ions on the degradation rate have been examined. A pseudo-first order kinetic model has been used to describe the results. A linear dependence of the rate constant upon the reciprocal of the initial 4-NP concentration has been obtained. The addition of $H_2O_2$ increases the reaction rate while $Cu^{2+}$ ions has a detrimental effect. With the intention of predicting the primary intermediates, geometry optimizations of the reactants, the products and the transition state complexes have been performed with the semi-empirical PM3 method. The molecular orbital calculations have been carried out by an SCF method using RHF or UHF formalisms. Based on the results of the quantum mechanical calculations, the rate constants of the two possible reaction paths have been calculated by means of the transition state theory, and 1,2-dihydroxy-4-nitro-cyclohexadienyl radical which then forms 4-nitrocatechol has been determined as the most probable primary intermediate by the application of three different theoretical shortcut methods. 

*Keywords:* Photocatalytic degradation; Titanium dioxide; Advanced oxidation; Semiconductor photocatalysis; 4-Nitrophenol

## 1. Introduction

Semiconductor photocatalysis is an advanced oxidation process to eliminate organic pollutants from water. In the last two decades, there have been a number of studies on this process, and it has recently been reviewed [1–3]. The semiconductor photocatalytic process is based on the combined use of low energy UV-A light and semiconductor photocatalysts of which the anatase form of $TiO_2$ is the most suitable [4,5].

When $TiO_2$, an n-type semiconductor is irradiated with light of wavelength $\lambda \leq 390$ nm, an electron jumps from the valence band (VB) to the conduction band (CB), leaving a hole behind. The electron–hole pairs, thus generated, are capable of initiating oxidation and reduction reactions on the surface of $TiO_2$ particles. In the presence of oxygen, these pairs migrate to the interface to yield oxidizing species. In aqueous suspension systems, holes ($h_{VB}{}^+$) react with surface $OH^-$ groups and produce $^\bullet OH$ radicals

$$h_{VB}{}^+ + OH^- \rightarrow {}^\bullet OH \quad (1)$$

radicals which are known to be the most oxidizing species [6–9], whereas electrons ($e_{CB}{}^-$) are trapped at surface defect sites, i.e. surface oxygen vacancies ($Ti^{3+}$) and removed by reactions with adsorbed molecular $O_2$ to produce

$$e_{CB}{}^- + O_2 \rightarrow O_2{}^{\bullet -} \quad (2)$$

produce superoxide anion radical, which then froms more $^\bullet OH$ radicals.

$$2O_2{}^{\bullet -} + 2H_2O \rightarrow 2{}^\bullet OH + 2OH^- + O_2 \quad (3)$$

The reactions of $^\bullet OH$ radicals with the organic pollutants lead to the mineralization of the compounds.

Phenol and its derivatives constitute an important class of water pollutants because of their stability and solubility in water. There are many conventional methods to destroy phenols, but each method has its shortcomings. Chemical oxidation methods are expensive and lead to the contamination of water with other toxic pollutants. The ozonation method is energy intensive and biodegradation can only be used for dilute wastewater [10,11]. Thus, semiconductor to photocatalysis seems to be more effective than the conventional to methods, because semiconductors are inexpensive and capable of mineralizing aromatic compounds. The photodegradation of phenol in $TiO_2$ suspensions have been studied by many investigators [7,9,10,12]. The results indicate

* Corresponding author. Fax: +90-212-449-15-14.
*E-mail address:* cinarz@yildiz.edu.tr (Z. Çınar).

1010-6030/02/$ – see front matter 
PII: S1010-6030(01)00620-7

that phenolic compounds decompose completely to $CO_2$ and $H_2O$ through a mechanism involving hydroxylation of the aromatic ring. Halogenated phenols have also been studied extensively. Usually, the first-order kinetic model has been used to describe the results. D'Oliveira et al. [6] have studied the photocatalytic degradation of a series of dichlorophenols and trichlorophenols and determined the intermediates experimentally by using their UV-spectra and mass-spectra. They have concluded that the intermediates all correspond to the hydroxylation of the aromatic ring and the substitution of the −OH group occurs at the *para* and/or *ortho* sites with respect to the original phenolic functionality. The photodegradation of 2- and 3-chlorophenol have been investigated and *para*-hydroxylation has been found out to be the main pathway for both of the compounds [11]. Stafford et al. [13] have examined the effects of $TiO_2$ loading and light conditions on the photocatalytic degradation of 4-chlorophenol and determined 4-chlorocatechol as the primary intermediate.

Nitrogen-containing phenols are also of great concern not only because they cause severe health problems but at the same time they are important poisons for catalysts [14]. However, there is very limited information on the kinetics and the reaction intermediates of the photocatalytic degradation of nitrogen-containing phenols [15,16].

In this study, 4-nitrophenol (4-NP) was chosen as the representative member of this pollutant group because of its environmental importance. 4-NP is toxic as are the other phenol derivatives. It is one of the 114 organic compounds listed by EPA. Its maximum allowed concentration in water is 20 ppb. Even if in very low concentrations, it causes chronic poisoning. 4-NP is used in the production of pesticides and synthetic dyes. It is also used as insecticides and herbicides. Since it has a significant water solubility, 1.6 g/100 ml, it is often present in wastewater discharges from such facilities. It may also be found in ground water wells and surface waters where it has to be removed in order to achieve drinking water quality.

In this paper, we present the results of our investigation on the photodegradation kinetics of 4-NP in aqueous $TiO_2$ suspensions. In the first part of the work, the effects of catalyst loading, initial concentration of 4-NP, the concentrations of $H_2O_2$ and the added $Cu^{2+}$ ions were determined experimentally. In the theoretical part, with the intention of predicting the types and the relative amounts of the primary intermediates, quantum mechanical calculations were carried out for all the possible reaction paths, and three different theoretical shortcut methods were applied.

## 2. Experimental details

### 2.1. Materials

The anatase form of $TiO_2$, Degussa P25 grade, with a particle size of 30 nm and a surface area of $50\,m^2\,g^{-1}$ was used as the photocatalyst without further treatment. All the chemicals that were used in the experiments were of laboratory reagent grade and used as received without further purification. The solutions were prepared with doubly-distilled water.

### 2.2. Photoreactor

The experiments were carried out in a batch-type photoreactor. The reactor consists of two parts. The first part is the outside metallic cylinder, which is 54.4 cm high and 31.6 cm in inside diameter. There are $5 \times 8$ W blacklight fluorescent lamps attached vertically onto the inner surface of the metallic cylinder at a distance of 12.0 cm apart from each other. At the bottom of the outer cylinder, there is a fan to cool the lamps. The second part of the reactor is a Pyrex glass cylinder which is 18.3 cm high and 9.0 cm in inside diameter with a volume of approximately 1000 ml and was used as the reaction vessel. The suspension was stirred magnetically throughout the reaction period in order to prevent $TiO_2$ particles from settlement. The incident light intensity was measured by means of a potassium ferrioxalate actinometer [17] and was found to be $3.1 \times 10^{-7}$ einsteins $s^{-1}$.

### 2.3. Experiments

In the experiments, a stock solution of 4-NP at a concentration of $1.0 \times 10^{-4}\,mol\,l^{-1}$ and at the natural pH (5.9) was used. The suspension was prepared by mixing definite volumes of this solution containing the desired amount of 4-NP with $TiO_2$. The suspension was agitated in an ultrasonic bath for 15 min in the dark before introducing into the photoreactor. The volume of the suspension was 600 ml. In the experiments, the amount of $TiO_2$ used was 0.3 g/100 ml which was determined as the optimum photocatalyst concentration. Owing to continuous cooling, the temperature of the reaction solution was $21 \pm 1\,^{\circ}C$. Under these conditions, the initial pH of the suspension was $5.1 \pm 0.2$ and measured by a pH meter, Metrohm E-510.

All the samples, each 10 ml in volume were taken intermittently for analysis. The samples were then filtered through 0.45 μm millipore discs. Before analyzing, all the solutions were wrapped with aluminum foil and kept in the dark. The concentration of 4-NP was measured with a Unicam UV–visible spectrophotometer. The calibration curves were prepared for a concentration range of $(1.0–10.0) \times 10^{-5}\,mol\,l^{-1}$ and the detection limit for 4-NP was calculated to be $1.94 \times 10^{-6}\,mol\,l^{-1}$. For the analysis of $Cu^{2+}$ ions, an atomic absorption spectrometer, Varian AA 10/20 AAS was used. In the experiments, the pH of the reaction solution decreased slightly. For 160 min of degradation, the change in the pH was 0.2–0.5 which did not affect the wavelength of maximum absorption in the UV spectrum of 4-NP.

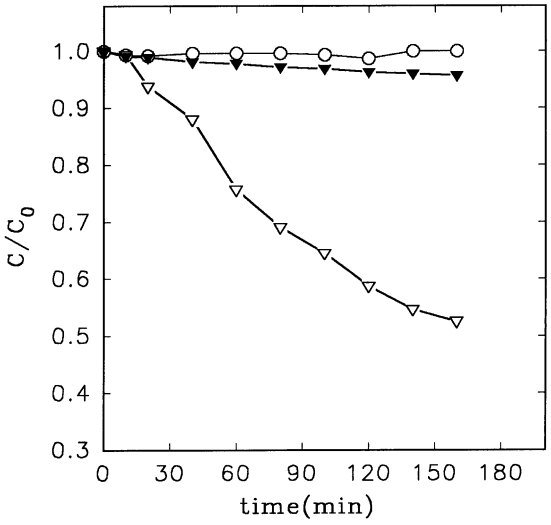


Fig. 1. Photocatalytic disappearance of 4-NP: (○) with light; (▼) with $TiO_2$; (▽) with $TiO_2$ + light.

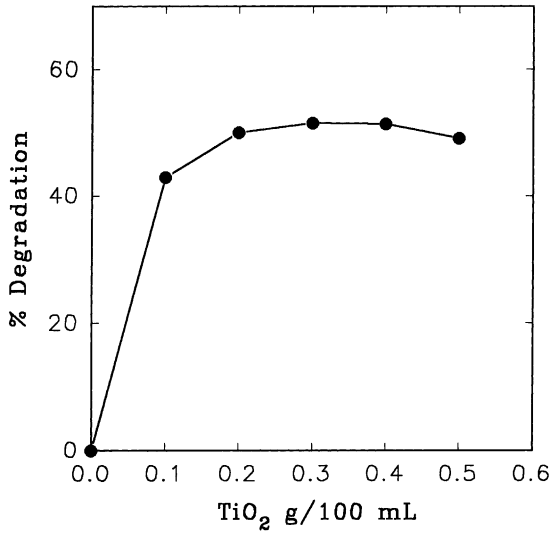


Fig. 2. Effect of $TiO_2$ loading on the photodegradation rate of 4-NP.

## 3. Results and discussion

### 3.1. Kinetics of 4-NP disappearance

Fig. 1 shows the kinetics of the disappearance of 4-NP from an initial concentration of $1.0 \times 10^{-4}$ mol l$^{-1}$ under three conditions. There was no observable loss of 4-NP when the irradiation was carried out in the absence of $TiO_2$. In non-irradiated suspensions, there was a slight loss, ca. 4.3%, due to adsorption onto $TiO_2$ particles. However, in the presence of $TiO_2$, a rapid degradation of 4-NP occurred by irradiation. The concentration change amounts to 58.7% after irradiating for 160 min.

The semi-logarithmic plots of concentration data gave a straight line. The correlation constant for the fitted line was calculated to be $r = 0.9943$. This finding indicates that the photocatalytic degradation of 4-NP in aqueous $TiO_2$ suspensions can be described by the first-order kinetic model, $\ln C = -kt + \ln C_0$, where $C_0$ is the initial concentration and $C$ is the concentration of 4-NP at time $t$. Under the experimental conditions used, the rate constant $k$ for the degradation of 4-NP was calculated to be $(4.27 \pm 0.16) \times 10^{-3}$ min$^{-1}$.

### 3.2. Effect of catalyst loading

Suspensions at pH $= 5.1 \pm 0.2$ and $1.0 \times 10^{-4}$ mol l$^{-1}$ 4-NP concentration were used to study the effect of catalyst loading by varying the amount of $TiO_2$ from 0.1 to 0.5 g/100 ml. The curve in Fig. 2 shows that without catalyst, the degradation of 4-NP is insignificant. As the concentration of $TiO_2$ increases, the rate of degradation increases up to a certain point, then begins to decrease slowly. Maximum degradation was obtained at a $TiO_2$ concentration of 0.3 g/100 ml. This observation indicates that beyond this optimum concentration, other factors affect the degradation of 4-NP. At high $TiO_2$ concentrations, particles aggregate which reduces the interfacial area between the reaction solution and the photocatalyst. Thus, the number of active sites on the catalyst surface is decreased. The increase in opacity and light scattering by the particles may be the other reasons for the decrease in the degradation rate.

### 3.3. Effect of initial concentration of 4-NP

The effect of initial concentration of 4-NP on the photocatalytic degradation rate was investigated over the concentration range of $(3.5–9.3) \times 10^{-5}$ mol l$^{-1}$, since the pollutant concentration is a very important parameter in water treatment. Experimental results are presented in Fig. 3

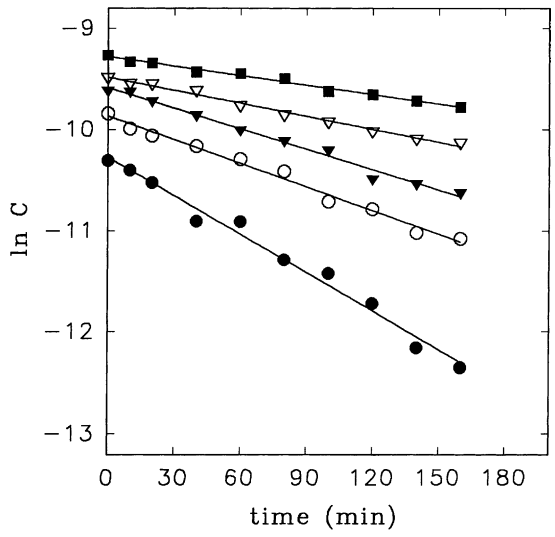


Fig. 3. Effect of initial concentration on the photodegradation rate of 4-NP: (■) $9.3 \times 10^{-5}$ mol l$^{-1}$; (▽) $7.6 \times 10^{-5}$ mol l$^{-1}$; (▼) $6.8 \times 10^{-5}$ mol l$^{-1}$; (○) $5.2 \times 10^{-5}$ mol l$^{-1}$; (●) $3.5 \times 10^{-5}$ mol l$^{-1}$.

Table 1
Effect of initial concentration of 4-NP on the photodegradation rate

| $C_0$ ($10^{-5}$ mol l$^{-1}$) | $k$ ($10^{-3}$ min$^{-1}$) | $r$ |
|---|---|---|
| 3.5 | 12.69 ± 0.53 | 0.9930 |
| 5.2 | 7.78 ± 0.30 | 0.9940 |
| 6.8 | 6.72 ± 0.26 | 0.9941 |
| 7.6 | 4.27 ± 0.16 | 0.9943 |
| 9.3 | 3.12 ± 0.13 | 0.9931 |

and Table 1, together with the correlation coefficients for each of the fitted lines. The results show that the degradation rate depends on the initial 4-NP concentration. The rate constant $k$ decreases with increase in the initial concentration of 4-NP. This finding indicates that the degradation kinetics of 4-NP is not of simple first order but pseudo-first order.

Furthermore, the slopes of the lines in Fig. 3 and the $k$ values in Table 1 show that the degradation rate decreases rapidly at low initial 4-NP concentrations. As the initial concentration increases, it begins to decrease slowly. As it can be seen from the values given in Table 1, the change in the rate constant is $4.91 \times 10^{-3}$ min$^{-1}$ when the initial 4-NP concentration increases from $3.5 \times 10^{-5}$ to $5.2 \times 10^{-5}$ mol l$^{-1}$. However, when the initial concentration increases from $7.6 \times 10^{-5}$ to $9.3 \times 10^{-5}$ mol l$^{-1}$, the decrease in the rate constant is much less, $1.15 \times 10^{-3}$ min$^{-1}$.

The initial concentration dependence of the photodegradation rate of 4-NP can be based on the fact that the degradation reaction occurs on $TiO_2$ particles as well as in solution [18]. On the surface of $TiO_2$ particles, the reaction occurs between the •OH radicals, generated at the active $OH^-$ sites and a 4-NP molecule from the solution. When the initial concentration is high, the number of these available active sites is decreased by 4-NP molecules, because of their competitive adsorption on $TiO_2$ particles. In this case, rate of transfer of 4-NP molecules from the solution does not affect the degradation rate. However, when the initial 4-NP concentration is low, transfer rate plays an important role. From Fig. 4, it can be seen that the degradation rate constants obtained in this study are proportional to the reciprocal of the initial 4-NP concentration. The correlation coefficient for the fitted line is 0.9849. Wei and Wan [9] have obtained a similar result for the photodegradation of phenol.

### 3.4. Effect of $H_2O_2$

The photocatalytic degradation of organic pollutants depends upon their reactions with the •OH radicals. Therefore, electron acceptors have been used to enhance the degradation rates since they generate •OH radicals [19–21]. $H_2O_2$ is the most widely used electron acceptor. The effect of $H_2O_2$ has been investigated in numerous studies and observed that it increases the photodegradation rates of organic pollutants [9,10,22]. The added $H_2O_2$ reacts with CB electrons to generate •OH radicals which are necessary for

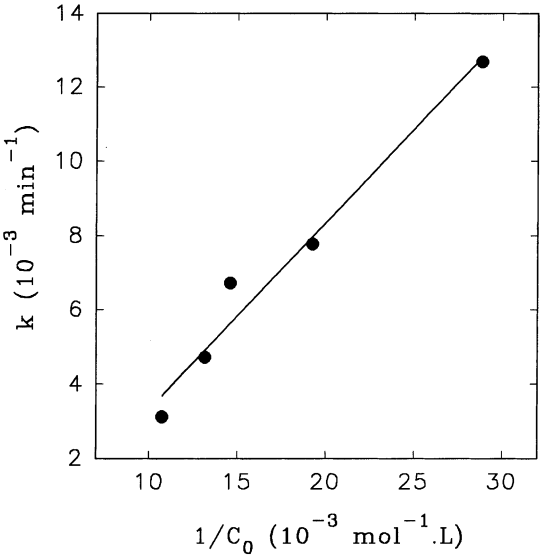


Fig. 4. Plot of the apparent rate constant vs. the reciprocal of the initial 4-NP concentration.

the photodegradation reactions

$$H_2O_2 + e_{CB}^- \rightarrow {}^{\bullet}OH + OH^- \quad (4)$$

Being an electron acceptor, $H_2O_2$ does not only generate •OH radicals, but it also inhibits electron–hole recombination process at the same time, which is one of the most important practical problems in using $TiO_2$ as a photocatalyst.

In this study, the variation in the photodegradation rate of 4-NP was determined as a function of $H_2O_2$ concentration [$H_2O_2$] over the range (2.0–10.0) $\times 10^{-4}$ mol l$^{-1}$ at pH = 5.1 ± 0.2 and at a constant temperature of 21 ± 1 °C by using suspensions at $1.0 \times 10^{-4}$ mol l$^{-1}$ 4-NP concentration. The results are presented in Fig. 5 and Table 2 with the

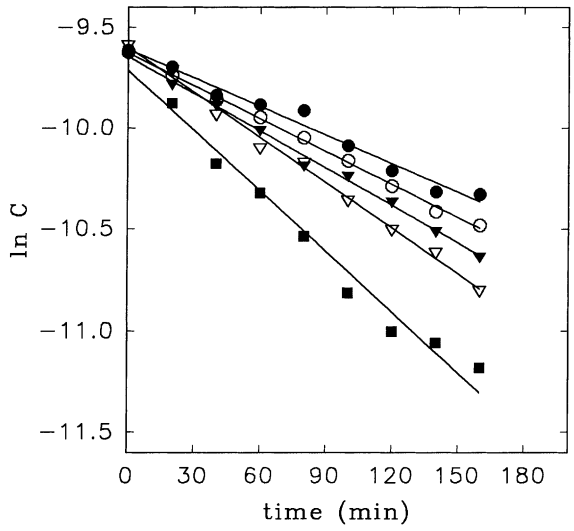


Fig. 5. Effect of $H_2O_2$ addition on the photodegradation rate of 4-NP: (●) $2.0 \times 10^{-4}$ mol l$^{-1}$; (○) $4.0 \times 10^{-4}$ mol l$^{-1}$; (▼) $6.0 \times 10^{-4}$ mol l$^{-1}$; (▽) $8.0 \times 10^{-4}$ mol l$^{-1}$; (■) $10.0 \times 10^{-4}$ mol l$^{-1}$.

Table 2
Effect of $H_2O_2$ addition on the photodegradation rate of 4-NP

| $[H_2O_2]$ ($10^{-4}$ mol l$^{-1}$) | $k$ ($10^{-3}$ min$^{-1}$) | $r$ |
|---|---|---|
| 0.0 | 4.27 ± 0.16 | 0.9943 |
| 2.0 | 4.73 ± 0.27 | 0.9892 |
| 4.0 | 5.44 ± 0.10 | 0.9989 |
| 6.0 | 6.15 ± 0.15 | 0.9981 |
| 8.0 | 7.47 ± 0.02 | 0.9973 |
| 10.0 | 9.95 ± 0.56 | 0.9890 |

correlation coefficients for each of the fitted lines. As it can be seen from the straight lines obtained, the photocatalytic degradation of 4-NP with the addition of $H_2O_2$ also follows the pseudo-first order kinetics. Furthermore, they also show that the addition of $H_2O_2$ enhances the degradation rate of 4-NP, as expected. The apparent rate constant was also found to be dependent upon the concentration of $H_2O_2$. The $k$ values, tabulated in Table 2, increase as the concentration of $H_2O_2$ increases. In order to find the order of $[H_2O_2]$ dependence of the photodegradation of 4-NP, the apparent rate constant was expressed as

$$k = k'[H_2O_2]^{\alpha} \quad (5)$$

in light of the results of an earlier work on the photodegradation of phenol [9]. The order of this dependence $\alpha$ was calculated to be 0.310 for the experimental range by linear regression. The correlation coefficient is $r = 0.9615$.

### 3.5. Effect of $Cu^{2+}$ ions

In recent years, addition of transition metal ions has been observed to increase the rate of $TiO_2$ photocatalytic degradation of organic pollutants [9,10,12,23–25]. This observed rate increase has been attributed to the behavior of the metal ions as electron scavangers. At the semiconductor surface, transition metal ions are reduced by the CB electrons through the following reaction:

$$M^{n+} + e_{CB}{}^{-} \rightarrow M^{(n-1)+} \quad (6)$$

where $M^{n+}$ represents $Fe^{3+}$, $Mn^{2+}$ and $Cu^{2+}$ which are the most widely studied metal ions to enhance the photocatalytic degradation rates. The above reaction prevents electron–hole recombination and results in an increased rate of formation of $^{\bullet}OH$ radicals. Photogenerated holes oxidize water molecules and surface hydroxyl groups to produce $^{\bullet}OH$ radicals

$$h_{VB}{}^{+} + H_2O \rightarrow {}^{\bullet}OH + H^{+} \quad (7)$$

$$h_{VB}{}^{+} + 2OH^{-} \rightarrow {}^{\bullet}OH + OH^{-} \quad (8)$$

Transition metal ions also increase the photodegradation rate by inducing photo-Fenton type reactions to produce more $^{\bullet}OH$ radicals [12,24].

$$M^{(n-1)+} + H_2O_2 + H^{+} \rightarrow M^{n+} + {}^{\bullet}OH + H_2O \quad (9)$$

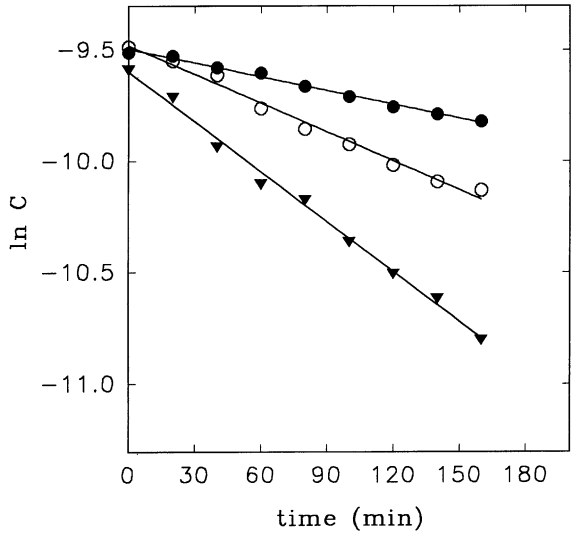


Fig. 6. Effect of $Cu^{2+}$ addition on the photodegradation rate of 4-NP: (●) 4-NP + $1.0 \times 10^{-3}$ mol l$^{-1}$ $Cu^{2+}$; (▼) 4-NP + $1.0 \times 10^{-3}$ mol l$^{-1}$ $H_2O_2$ (○) 4-NP.

The effect of $Fe^{3+}$ ions on the photodegradation of organic compounds has been investigated extensively. It has been found out that trace amounts of ferric ions increases the degradation rate up to a certain $Fe^{3+}$ concentration, then the rate begins to decrease. Excessive ferric ions tend to retard this catalytic effect [9,10,12,24]. $Mn^{2+}$ ions have been reported to affect the photodegradation reactions of organic pollutants positively [24]. However, there is a considerable controversy in the results obtained showing the effect of cupric ions $Cu^{2+}$. Some of the investigators [23–25] have found that cupric ion behaves as an accelerator, whereas some others [9,10] have obtained a decrease in the apparent rate constant upon the addition of $Cu^{2+}$ ions.

In this study, the effect of $Cu^{2+}$ ions on the photodegradation rate of 4-NP was investigated by using suspensions at $1.0 \times 10^{-4}$ mol l$^{-1}$ 4-NP concentration. The concentration of $Cu^{2+}$ ions was $1.0 \times 10^{-3}$ mol l$^{-1}$ and the initial pH of the reaction solution was 5.1 ± 0.2. The experimental results are presented in Fig. 6 and Table 3. For comparison, the results obtained for the photodegradation of 4-NP alone and in the presence of $1.0 \times 10^{-3}$ mol l$^{-1}$ $H_2O_2$ with the initial concentration of $1.0 \times 10^{-4}$ mol l$^{-1}$ are also given. The results show that the photocatalytic degradation of 4-NP with the addition of $Cu^{2+}$ ions also follows the pseudo-first order kinetics. It can be seen from the values in Table 3 that the

Table 3
Effect of $Cu^{2+}$ ions on the photodegradation rate of 4-NP

| Initial conditions[a] | $k$ ($10^{-3}$ min$^{-1}$) | $r$ |
|---|---|---|
| 4-NP | 4.27 ± 0.16 | 0.9943 |
| 4-NP + $1.0 \times 10^{-3}$ mol l$^{-1}$ $H_2O_2$ | 9.95 ± 0.56 | 0.9890 |
| 4-NP + $1.0 \times 10^{-3}$ mol l$^{-1}$ $Cu^{2+}$ | 2.08 ± 0.07 | 0.9960 |

[a] Initial concentration of 4-NP is $1.0 \times 10^{-4}$ mol l$^{-1}$.

addition of $Cu^{2+}$ ions causes a decrease in the apparent rate constant from $4.27 \times 10^{-3}$ to $2.08 \times 10^{-3}\,min^{-1}$, but $k$ value increases to $9.95 \times 10^{-3}\,min^{-1}$ with the addition of $H_2O_2$.

The reason for this observed negative effect of $Cu^{2+}$ ions on the photocatalytic degradation of 4-NP may be attributed to the low reduction potential for $Cu^{2+}/Cu^{1+}$ couple. This value is −0.1 eV with respect to NHE [25]. As a result, $Cu^{2+}$ ions are reduced to $Cu^{1+}$ by CB electrons

$$Cu^{2+} + e_{CB}{}^{-} \rightarrow Cu^{1+} \quad (10)$$

while $Cu^{1+}$ ions thus formed are oxidized to $Cu^{2+}$ by the photogenerated holes on the surface of $TiO_2$ particles or by $^{\bullet}OH$ radicals through the following reactions:

$$Cu^{1+} + h_{VB}{}^{+} \rightarrow Cu^{2+} \quad (11)$$

$$Cu^{1+} + {}^{\bullet}OH + H^{+} \rightarrow Cu^{2+} + H_2O \quad (12)$$

Therefore, the above explained $Cu^{2+} \leftrightarrow Cu^{1+}$ cycle does not produce any $^{\bullet}OH$ radicals and furthermore, it causes a decrease in the concentration of the $^{\bullet}OH$ radicals present in the photocatalytic system. Thus, we may conclude that $Cu^{2+}$ has a negative effect on the photodegradation reaction of 4-NP.

### 3.6. Theoretical prediction of the primary intermediates

The photodegradation reactions of organic pollutants may take place through the formation of harmful intermediates that are more toxic than the original compounds. Therefore, the knowledge on the identities of the intermediates is a necessity in photocatalytic degradation processes. In aqueous $TiO_2$ suspensions, aromatic compounds are oxidized through two different mechanisms; either by hydroxylation of the aromatic ring [6–9,11] or by direct electron transfer to $TiO_2$ followed by the addition of a water molecule and loss of a proton [26–28]. In both of the reaction paths, a hydroxycyclohexadienyl type radical is formed; therefore, the photocatalytic degradation of 4-NP may be based on hydroxyl radical chemistry.

In this study, in order to predict the primary intermediates, the kinetics of the hydroxylation reaction of 4-NP was investigated theoretically. Hydroxyl radical has a strong electrophilic character [29,30], it attacks to one of the carbon atoms of the aromatic ring, generally the one with the highest electron density. Two different reaction paths for the hydroxylation of 4-NP were determined by the nature of the carbon atoms of the aromatic ring. In both of the two possible reaction paths, shown in Fig. 7, the $^{\bullet}OH$ radical attacks a carbon atom with its unpaired electron and upon contact forms a C–O bond, while a π-bond of the aromatic ring is broken and a hydroxylated radical is formed. The equilibrium structures, electronic and thermodynamic properties of the reactants, 4-NP and $^{\bullet}OH$, the products, two different hydroxylated radicals formed and the corresponding transition state TS structures were evaluated by quantum mechanical calculations.

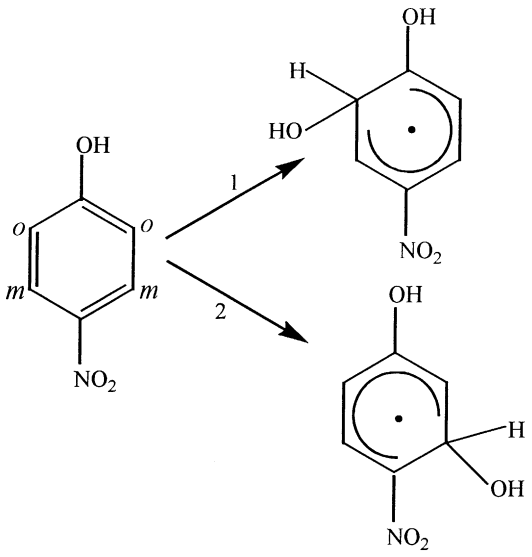


Fig. 7. Possible reaction paths for the hydroxylation of 4-NP.

#### 3.6.1. Molecular orbital calculations

Geometry optimizations were performed with the semiempirical PM3 method within the MOPAC 6.0 package [31]. The molecular orbital calculations were carried out by a self-consistent field SCF method using the restricted RHF or unrestricted UHF Hartree–Fock formalisms, depending upon the multiplicity of each species. The molecular models were created by using the mean bond distances, the geometric parameters of the benzene ring, tetrahedral angles 109.5° for $sp^3$-hybridized oxygen and carbon atoms and 120° for $sp^2$-hybridized carbons and nitrogen. In the calculation of the hyroxylated radicals, the aromatic ring was left undisturbed and the attacking $^{\bullet}OH$ radical was assumed to form a tetrahedral angle with the C–H bond. These structures were the input coordinates for PM3 calculations. The criterion for terminating all optimizations was increased by using the PRECISE option. Vibrational frequencies were calculated for the determination of the reactant and the product structures as stationary points and true minima on the potential energy surfaces using the keyword FORCE. All the stationary points were confirmed by the presence of positive vibrational frequencies. For a stationary point, the first derivatives of the energy with respect to changes in the geometry are zero. Whereas, the criterion for a minimum is that all eigenvalues of the Hessian matrix are positive [32]. The forming C–O bond was chosen as the reaction coordinate in the determination of the transition states and each transition state was characterized with only one negative eigenvalue in its force constant matrix.

#### 3.6.2. Frontier orbital theory

As explained above, $^{\bullet}OH$ radicals react with aromatic molecules through addition to yield hydroxycyclohexadienyl type radicals. There are several theoretical shortcut methods in the literature for the determination of the position

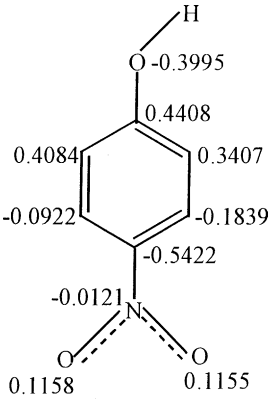


Fig. 8. HOMO coefficients for 4-NP.

of attack of the •OH radical in such reactions [30]. One of the most successful ones is the "frontier orbital theory" which states that in electrophilic reactions, the point of attack is at the position of the greatest electron density in the HOMO (highest occupied molecular orbital) of the aromatic molecule. In the case of a highly electrophilic radical such as •OH, the SOMO (singly occupied molecular orbital) of the radical and the HOMO of the aromatic molecule overlaps. The •OH radical has a very low-lying SOMO, the energy of which was calculated to be −12.537 eV. The energies of the HOMO and LUMO (lowest unoccupied molecular orbital) of 4-NP were found to be −10.169 and −1.081 eV, respectively. Therefore, in the hydroxylation of 4-NP, the SOMO of the •OH radical interacts with the HOMO of 4-NP. The HOMO coefficients for 4-NP obtained in this study are shown in Fig. 8. The values indicate a high preference for the two *-ortho* positions with respect to the functional −OH group. But, path 1 is the most preferable reaction path. The most interesting feature of Fig. 8 is the high HOMO coefficients on the oxygen and the two substituted carbon atoms. This may lead one to think that the attack is on the oxygen atom or the two substituted carbon atoms. But there is an experimental evidence that •OH radicals attack aromatic molecules at the ring positions. For the two substituted carbon atoms, there is a steric hinderance which may cause an increase in the activation energy of the reaction.

Table 4
Total energies and heats of formation of the intermediates

| Path | $E$ (au) | $\Delta H_f$ (kcal mol$^{-1}$) |
|---|---|---|
| 1 | −78.526 | −62.282 |
| 2 | −78.520 | −58.623 |

### 3.6.3. Wheland's approach

Another theory for the determination of the position of attack of the •OH radical to the aromatic molecule is the localization approach of Wheland [30]. According to this theory, the position of attack is determined by the energy of the intermediate. The total energies $E$ and the heats of formation $\Delta H_f$ of the two hydroxylated radicals calculated in this study are tabulated in Table 4. As it can be seen from the values given, the lowest $E$ and $\Delta H_f$ belong to the radical formed in path 1, indicating that the attack is at the *-ortho* position. Thus, the frontier orbital theory and the localization approach gave the same prediction; path 1 is the most probable. But, in order to be sure of this prediction, we examined the TS structures and calculated the kinetic parameters for the two reaction paths.

### 3.6.4. Transition state structures

The optimized structures obtained for the two transition states, together with the important structural parameters are presented in Fig. 9. It was observed that the major structural changes relative to 4-NP are all localized around the carbon atom to which the •OH radical attacks. Upon the approach of the •OH radical, this carbon atom moves slightly out of the plane of the ring. The dihedral angles calculated are 1.2° and 1.9°. The coming oxygen atom makes a 102.6–104.5° angle with the C–C bond, while the hydrogen atom bonded to the carbon atom to which the •OH radical attacks moves out of the plane of the ring. The dihedral angles calculated

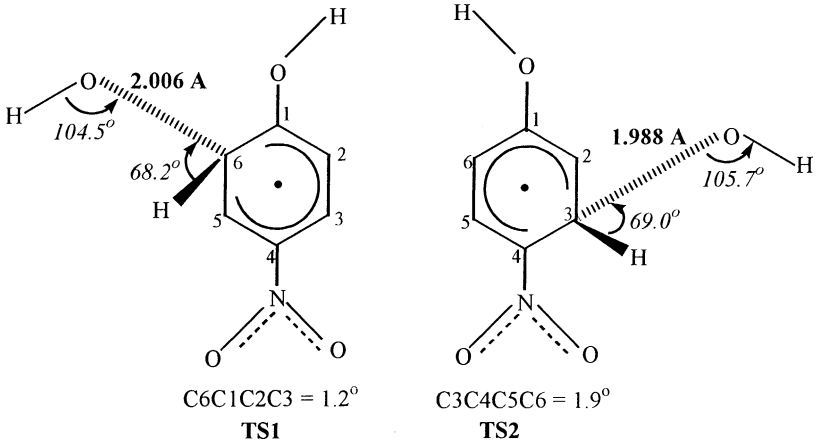


Fig. 9. Optimized structures for the transition states.

Table 5
Predictors for the determination of the most probable TS

| TS | C–O (Å) | $n_{C–O}$ | $\Delta H_f$ (kcal mol$^{-1}$)[a] |
|---|---|---|---|
| TS1 | 2.006 | 0.180 | −22.951 |
| TS2 | 1.988 | 0.192 | −22.223 |

[a] The values are for $T = 300$ K.

for the hydrogen atom are greater than the ones obtained for the carbon atom, 6.4–7.8°. These findings indicate that the carbon atom to which the •OH radical is being bonded changes from $sp^2$ to $sp^3$ hybridized.

In this study, three predictors were determined for the prediction of the most probable TS; the length of the forming C–O bond, its bond order $n_{C–O}$ and the heats of formation $\Delta H_f$ of the TS. They are presented in Table 5. The C–O bond length is a sensitive measure for the formation of the transition state along the reaction coordinate. As it can be seen from the values given in Fig. 9 and Table 5, the longest C–O bond belongs to TS1. This suggests that TS1 is the earliest transition state and is in clear agreement with the smallest bond order which is 0.180 as presented in Table 5. Furthermore, TS1 has the lowest heat of formation, indicating that it is thermodynamically more stable. Thus, we may say that TS1 is the most probable transition state.

### 3.6.5. Transition state theory

The rate constant $k$ for each reaction path was calculated by using the transition state theory over a temperature range 200–400 K. The classical rate constant $k$ in transition state theory is

$$k = \frac{kT}{h}\frac{q_{TS}}{q_{NP}q_{OH}}e^{-Ea/RT} \quad (13)$$

where k is the Boltzman's constant, $T$ the temperature, $h$ the Planck's constant, $q$ the molecular partition functions for TS and the reactant species, 4-NP and •OH, and $E_a$ the activation energy. Each of the molecular partition functions was assumed to be the product of translational, rotational, vibrational and electronic partition functions of the corresponding species. The activation energies for the two reaction paths were calculated as the difference between the heats of formation of the transition state complexes and the sum of the heats of formation of the reactants. The calculated rate constants $k$, activation energies $E_a$ and heats of reaction $\Delta H_r$, calculated as the sum of the heats of formation of the products minus the sum of the heats of formation of the reactants are presented in Table 6. As it can be seen from the values, the lowest activation energy belongs to path 1 for which the position of attack

Table 6
Kinetic parameters for the two possible reaction paths[a]

| Path | $E_a$ (kcal mol$^{-1}$) | $k$ (cm$^3$ (molecule s)$^{-1}$) | $\Delta H_r$ (kcal mol$^{-1}$) |
|---|---|---|---|
| 1 | 5.825 | $1.270 \times 10^{-13}$ | −33.506 |
| 2 | 6.553 | $1.127 \times 10^{-15}$ | −29.847 |

[a] All the values are for $T = 300$ K.

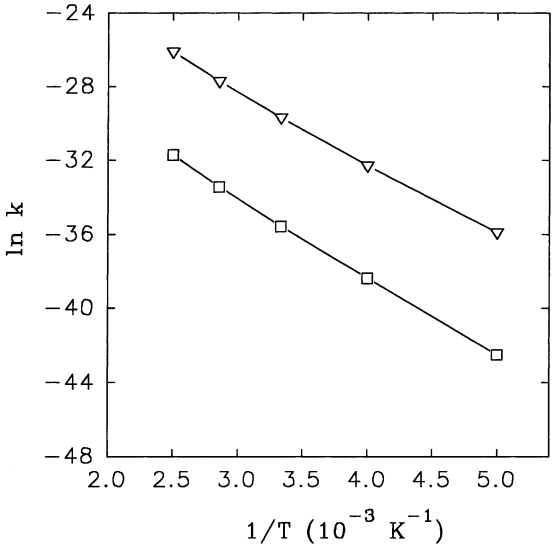


Fig. 10. Arrhenius plots for the two possible reaction paths: (▽) path 1; (□) path 2.

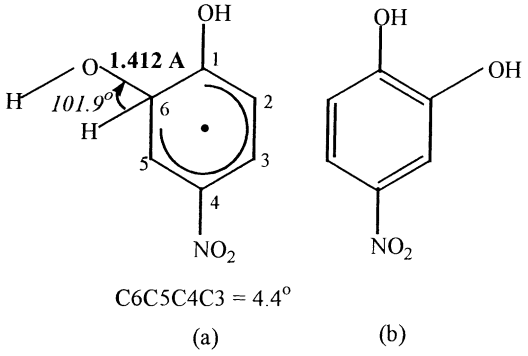


Fig. 11. Primary intermediates of the photodegradation of 4-NP.

is at the *ortho*-carbons. Moreover, the highest exothermicity and the highest rate constant belong to path 1. This result is consistent with Hammond's postulate [33], stating that early transition states have low energy barriers and high exothermicities. Arrhenius plots of the two possible paths, shown in Fig. 10, also support this finding. Path 1 proceeds faster than the other reaction path. This result is in agreement with the former two predictions. Thus, we may conclude that the most probable primary intermediate that forms in the photodegradation of 4-NP is 1,2-dihydroxy-4-nitro-cyclohexadienyl radical which then forms 4-nitrocatechol, shown in Fig. 11a and b, respectively. The relative concentration of this product was calculated to be 99.1%, which is in accordance with the experimental results reported in literature [15,16].

## 4. Conclusion

The results of this study show that the photocatalytic degradation of 4-NP in aqueous $TiO_2$ suspensions follows

a pseudo-first order kinetics. The apparent rate constant depends on the initial 4-NP concentration. A linear dependence of the rate constant upon the reciprocal of the initial 4-NP concentration has been obtained. The addition of $H_2O_2$ increases the reaction rate significantly depending upon its concentration, while the addition of $Cu^{2+}$ ions has a detrimental effect on the degradation rate. The order of the dependence of the rate constant on $H_2O_2$ concentration has been calculated to be 0.310. Based on the results of the quantum mechanical calculations, the most probable primary intermediate has been determined to be 1,2-dihydroxy-4-nitro-cyclohexadienyl radical which then forms 4-nitrocatechol.

## Acknowledgements

The authors greatly appreciate Yıldız Technical University Research Fund for financial support (Project No.: 20-01-02-03) and Degussa Limited Company Turkey for the generous gift of $TiO_2$ P25.

## References

[1] A. Mills, S. Le Hunte, J. Photochem. Photobiol. A 108 (1997) 1.
[2] D. Bahnemann, J. Cunningham, M.A. Fox, E. Pelizzetti, P. Pichat, N. Serpone, in: G.R. Helz, R.G. Zepp, D.G. Crosby (Eds.), Aquatic and Surface Photochemistry, Lewis, Baco Raton, FL, 1994, p. 261.
[3] P. Pichat, in: G. Ertl, H. Knözinger, J. Weitkamp (Eds.), Handbook of Heterogeneous Photo-catalysis, Vol. 4, VCH, Weinheim, 1997, p. 2111.
[4] D.F. Ollis, E. Pelizzetti, N. Serpone, Environ. Sci. Technol. 25 (9) (1991) 1523.
[5] D.W. Bahnemann, D. Bockelmann, R. Goslich, Sol. Energy Mater. 24 (1991) 564.
[6] J.C. D'Oliveira, C. Minero, E. Pelizzetti, P. Pichat, J. Photochem. Photobiol. A 72 (1993) 261.
[7] R.W. Matthews, S.R. Mcevoy, J. Photochem. Photobiol. A 64 (1992) 231.
[8] S. Das, M. Muneer, K.R. Gopidas, J. Photochem. Photobiol. A 77 (1992) 83.
[9] Y.T. Wei, C. Wan, J. Photochem. Photobiol. A 69 (1992) 241.
[10] Y.T. Wei, Y.Y. Wang, C. Wan, J. Photochem. Photobiol. A 55 (1990) 115.
[11] J.C. D'Oliveira, G. Al-Sayyed, P. Pichat, Environ. Sci. Technol. 24 (1990) 990.
[12] A. Sclafani, L. Palmisano, E. Davi, J. Photochem. Photobiol. A 56 (1991) 113.
[13] U. Stafford, K.A. Gray, P. Kamat, J. Catal. 167 (1997) 25.
[14] A. Huang, L. Cao, J. Chen, F.J. Spiess, S.L. Suib, T.N. Obee, S.O. Hay, J.D. Freihaut, J. Catal. 188 (1999) 40.
[15] M.S. Dieckmann, K.A. Gray, Wat. Res. 30 (1996) 1169.
[16] D. Chen, A.K. Ray, Wat. Res. 32 (1998) 3223.
[17] J.G. Calvert, J.N. Pitts, Photochemistry, Wiley, New York, 1966, pp. 783–786.
[18] H. Al-Ekabi, P. De Mayo, J. Phys. Chem. 90 (1986) 4075.
[19] H. Al-Ekabi, B. Butters, D. Delary, J. Ireland, N. Lewis, T. Powell, J. Story, in: D.F. Ollis, H. Al-Ekabi (Eds.), Photocatalytic Purification and Treatment of Water and Air, Elsevier, Amsterdam, 1993, pp. 321–335.
[20] I. Paulios, I. Tsachpinis, J. Chem. Technol. Biotechnol. 74 (1999) 349.
[21] L. Sanchez, J. Peral, X. Domenech, Appl. Catal. B 19 (1998) 59.
[22] M. Halmann, J. Photochem. Photobiol. A 66 (1992) 215.
[23] M. Bideau, B. Claudel, L. Faure, H. Kazaoun, J. Photochem. Photobiol. A 61 (1991) 269.
[24] E.C. Butler, A.P. Davis, J. Photochem. Photobiol. A 70 (1993) 273.
[25] N.S. Foster, R.D. Noble, C.A. Koval, Environ. Sci. Technol. 27 (1993) 350.
[26] R.B. Draper, M.A. Fox, Langmuir 6 (1990) 1396.
[27] G. Lu, A. Linsebigler, J.T. Yates Jr., J. Phys. Chem. 99 (1995) 6726.
[28] L. Cermanati, P. Pichat, C. Guillard, A. Albini, J. Phys. Chem. B 101 (1997) 2650.
[29] V. Brezova, M. Ceppan, E. Brandsteterova, M. Breza, L. Lapcik, J. Photochem. Photobiol. A 59 (1991) 385.
[30] M.K. Eberhardt, M. Yoshida, J. Phys. Chem. 77 (1973) 589.
[31] J.P. Stewart, MOPAC QCPE Program, 455, Bloomington Ind., 1990.
[32] M.W. Jurema, G.C. Shields, J. Comp. Chem. 14 (1) (1973) 89.
[33] W.J. Hehre, L. Radom, P.R. Schleyer, J.A. Pople, Ab Initio Molecular Orbital Theory, Wiley, New York.